

GIS MAPPING OF LANDSLIDE SUSCEPTIBILITY AND LIFE RISK IN BLUE MOUNTAINS NATIONAL PARK

Zack Tuckey

Jacobs Group (Australia) Pty Ltd

ABSTRACT

Blue Mountains National Park is part of a world heritage-listed conservation area managed by New South Wales National Parks and Wildlife Service, spanning over one million hectares of protected wilderness on the western outskirts of Sydney. The park encompasses an uplifted tableland of Triassic sandstone, underlain by shale, claystone, and coal measures. The escarpment is incised by rivers and streams, forming deep valleys surrounded by cliffs. Some of the most popular walking tracks receive hundreds of thousands of annual visitors and follow steep routes that connect the top of the escarpment to the valleys below via switchbacks, stairways and ladders that pass under high cliffs and overhangs. Typically, a new rockfall or debris slide is reported in the park about once per month, and over the last decade, landslides have infrequently caused serious injuries and fatalities; more frequently, they have caused major damage to walking tracks and fire trails.

Previous landslide risk assessments in the park have usually been focused on life risk for bushwalkers, with assessments undertaken on a site-specific basis in response to past instability or incipient slope failure. Under the National Parks *Landslides and Rockfalls Procedures*, the results of quantified risk assessments are used to estimate societal risk and develop appropriate risk mitigation strategies. Despite many years of reactive and site-specific landslide risk assessment, the park contains hundreds of kilometres of trails and walking tracks, and many locations have never been subject to any form of landslide risk assessment. This paper presents methods and findings of a proactive GIS investigation of landslide susceptibility and risk across 3400 km² of Jamison and Grose Valley, encompassing the most visited regions of the park. A landslide susceptibility map was produced from analysis of digital elevation models, expected rainfall intensity, bedrock geology, and hillslope erosion datasets. The concept of a “synthetic landslide return period” is introduced to link GIS-based landslide susceptibility scores to potential life risk for track and road users. The resulting susceptibility and risk maps can be interrogated to rank the relative landslide risk exposure of linear infrastructure, and identify locations that may require additional administrative risk management, site investigation, or engineered slope risk mitigation works.

1 INTRODUCTION

Blue Mountains National Park is one of the most visited bushwalking destinations in Australia, located on the western margin of the Sydney Basin. The park is managed by the New South Wales National Parks and Wildlife Service (NPWS) and contains hundreds of kilometres of walking tracks and fire trails; the most popular tracks receive hundreds of thousands of annual visitors and traverse under high sandstone cliffs and across steep terrain subject to frequent rockfall and landslides. In 2019 NPWS first published landslide risk management procedures based on the quantitative risk assessment (QRA) framework of the Australian Geomechanics Society (2007). When landslide hazards pose an unacceptable societal risk to life, NPWS seeks to mitigate the risk in accordance with the *ALARP* principle, which tests whether risks have been reduced *as low as reasonably practicable*, such that the level of risk reduction is proportionate to the cost and environmental impact of the works, as well as the safety risks faced by workers undertaking remediation activities. Until recently, landslide hazards in the park have usually been managed using a reactive approach, with site-specific investigations undertaken in response to new or incipient slope instability.

Decades of local NPWS staff experience have produced a good understanding of the slope failure mechanisms and frequency of instability for some of the most landslide-prone locations in the park. Despite this extensive institutional experience, many locations have never been subject to formal landslide risk assessment. Following an internal review of landslide risk, NPWS commissioned a proactive GIS study to investigate spatial trends in landslide susceptibility and risk across a 3400 km² region spanning most of Jamison Valley and Grose Valley. The primary goal of the study was to develop a GIS methodology that could be used to rank the relative landslide risk exposure for all walking tracks and fire trails using a standardised approach, allowing for direct comparison and ranking of assets by relative landslide risk exposure. The outputs of the study included a GIS “heat map” of landslide susceptibility, with walking tracks and fire trails divided into 10 m long sections and colour-coded according to a series of derived measures for landslide susceptibility and life risk.

This paper describes the GIS mapping methodology, tailored to the geological setting of the Blue Mountains, and introduces the concept of a “synthetic landslide return period” that links landslide susceptibility to annualised life risk. The resulting GIS “heat map” and colour-coded track alignments provide a useful tool to visualize the spatial variation in

landslide risk across multi-kilometre tracks and trails that traverse across variable terrain, and the entire GIS database is hosted on a web viewing platform to allow NPWS to interrogate the dataset and generate customised map sheets. The “synthetic return period” approach provides a semi-quantitative assessment of relative life risk that, over time, can be benchmarked against empirical landslide magnitude-frequency records collected by NPWS, increasing confidence in the critical QRA parameter P_H which represents the estimated annual probability of landslide initiation.

2 LANDSLIDES IN BLUE MOUNTAINS NATIONAL PARK

2.1 GEOLOGICAL AND PHYSIOGRAPHIC SETTING

The Blue Mountains are an uplifted sandstone tableland that has been deeply incised by rivers and creeks, with cliff up to 200 m high surrounding the Jamison and Grose Valleys. The communities of Katoomba and Blackheath are built on top of the uplifted sandstone plateau, with park visitors typically accessing Jamison Valley and Grose Valley by descending steep switchbacks, fabricated metal and carved bedrock stairways that connect the top of the escarpment to the valley trails below. The topography of the park is dominated by prominent escarpment cliffs. Figure 1 shows an isometric view of the publicly available 2 m resolution digital elevation model (DEM) near Katoomba, coloured by slope angle. A continuous 18 km stretch of walking tracks traverses across the steep upper talus slopes and along the base of the cliffs between Narrow Neck in the west and Wentworth Falls in the east. The slope gradient decreases with distance away from the upper cliffs, before descending into the nested v-shaped valleys of Govetts Leap Creek in the Grose Valley and Kedumba River in the Jamison Valley, which have eroded beneath the Illawarra Coal Measures and into Shoalhaven Group, which forms the basal unit of the Sydney Basin.

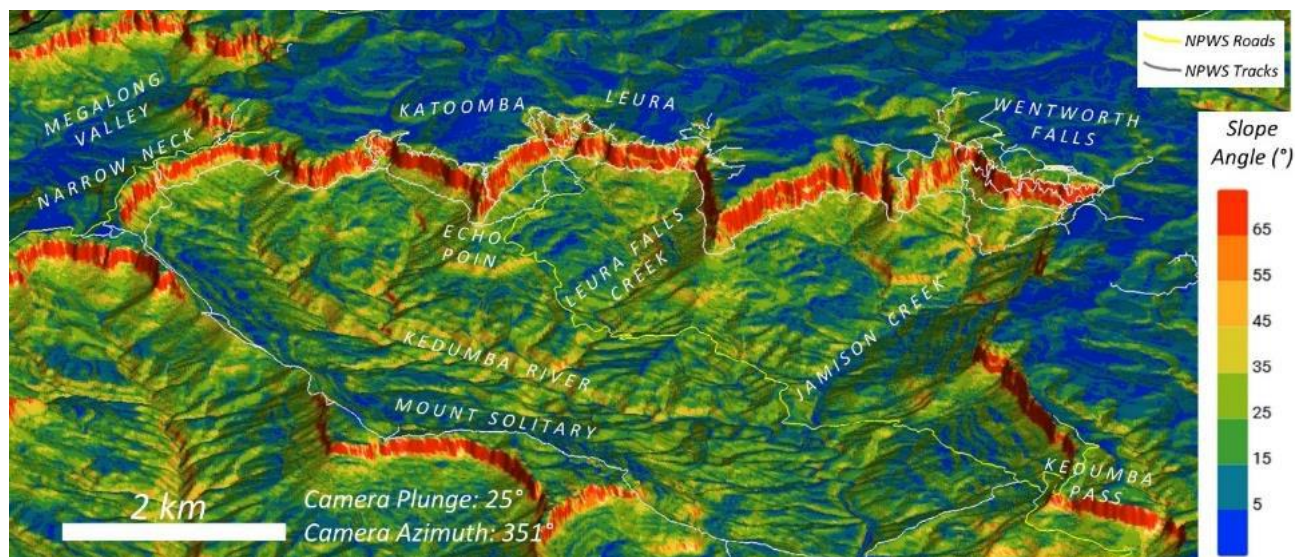


Figure 1: Isometric view of regional elevation model centred on Jamison Valley, coloured by slope angle

The network of valley trails includes many routes that traverse along the base of the sandstone cliffs within the “rockfall shadow” of the escarpment. Figure 2 shows an interpreted cross section and annotated photogrammetry image highlighting the key geological units and walking tracks that traverse across the cliffs near Wentworth Falls. Zones of geologically frequent rockfall are inferred from the presence of overhangs and pale, fresh sandstone.

The upper cliffs are comprised of the massive, quartzose Banks Wall Sandstone of the Narrabeen Group, which is locally up to 120 m thick. The Banks Wall Sandstone is underlain by the Mount York Claystone, a marker unit of weak, red-brown claystone that that forms a continuous bench in the middle of the cliffs that can be traced for kilometres across the escarpment. The lower cliffs are formed by the Burra-Moko Head Sandstone, an early Triassic quartzose to quartz-lithic sandstone that is up to 110 m thick, underlain by interbedded claystone, shale, and quartz-lithic sandstone of the Caley Formation, which forms the basal unit of the Narrabeen Group and the Permian-Triassic boundary. The late Permian Illawarra Coal Measures outcrop at the base of the cliffs, comprising coal seams, torbanite (oil shale), siltstone, and minor sandstone layers. Through the late 1800s and into the early 1900s numerous underground mining operations extracted torbanite and coal from these formations using the room and pillar technique, producing extensive networks of mine workings more than 200 m below the crest of the escarpment. Underground coal mining operations have been associated with major cliff collapses at various locations throughout the Blue Mountains including at the Newnes oil shale mine between 1911 and 1915 (Pells et al., 1987), the Dogface Rock landslide of 1931 above the Katoomba Colliery (Tuckey, 2023) and more recent failures at Nattai North Colliery in the 1960s and 1970s (Cunningham, 1988).

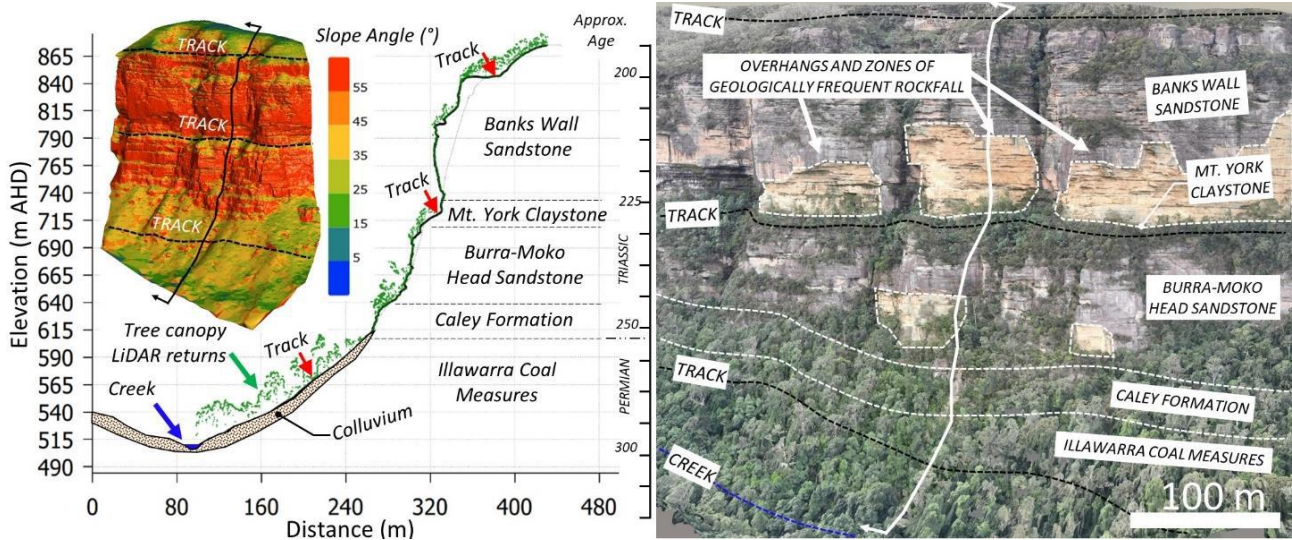


Figure 2: Interpreted LiDAR cross section and photogrammetry imagery of the cliffs near Wentworth Falls

The next section presents examples of typical landslide mechanisms observed throughout the park.

2.2 ESCARPMENT RETREAT AND LANDSLIDE MECHANISMS

Following uplift of the Blue Mountains during the late Triassic, the geomorphic processes shaping the landscape have been dominated by erosion by stream incision and gravity-driven slope failures. Rockfalls are ubiquitous along the escarpment cliffs, being products of the long-term processes of valley incision and escarpment retreat that have produced the modern landscape. Figure 2 shows the conceptual sequence of v-shaped valley incision into Jamison Valley, occurring due to the variations in rock mass strength between the stronger Narrabeen group sandstones at the top of the escarpment and the weaker underlying Illawarra Coal Measures, Shoalhaven Group, and Devonian basement rocks.

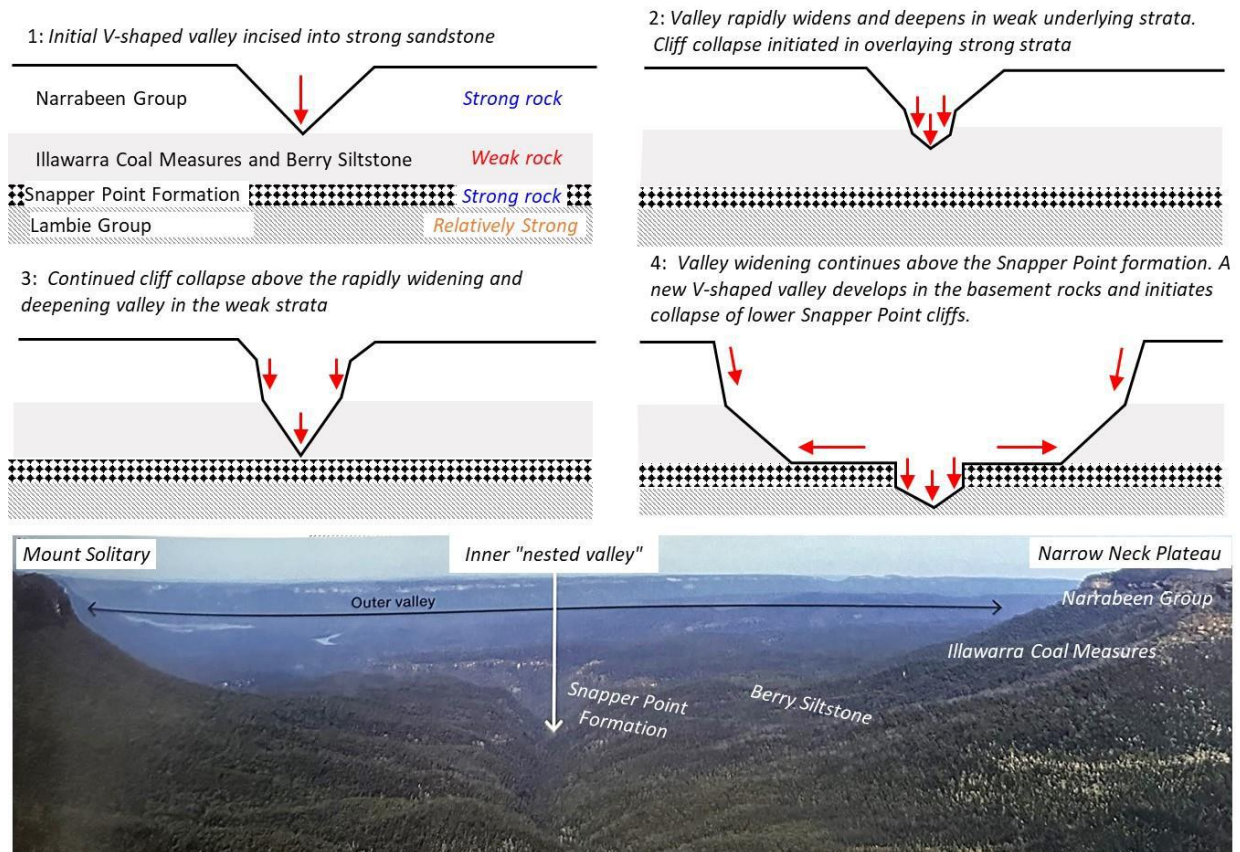


Figure 3: Formation of nested river valleys in the Jamison Valley (modified after Hatherly and Brown, 2022)

NPWS records and area staff experience suggest that the most common landslide types in the Blue Mountains include (1) **rockfalls and topples** initiating from the sandstone cliffs, varying in scale from discrete failure of centimetre-scale blocks, up to rock mass-scale cliff collapse events; (2) **debris slides** initiating on steeper sections of the colluvial talus slopes and valley rim (typically involving basal shearing along the interface between soil and bedrock driven by intense or prolonged rainfall); and (3) channelised **debris flows** that initiate along the upper slopes of the valley rims, with runout along creeks or ephemeral drainage lines, usually triggered by short intense rainfall events.

Rockfalls in the Narrabeen Group sandstone rocks often involve failure of overhanging or undermined blocks of sandstone. Two regionally ubiquitous vertical joint sets interact with subhorizontal bedding to produce cubic to tabular-shaped blocks that are kinematically free to detach from the cliffs. Failure is promoted by the preferential erosion of weak shale and claystone layers that degrade with cyclical changes in moisture content. Where tracks pass directly under natural or excavated overhangs, blocks may freefall just a few metres directly onto the track; other rockfalls have involved long runout of blocks onto tracks that traverse the valley slopes below the base of the cliffs. Rockfall initiation may be promoted by tree root jacking, elevated pore pressures from intense rainfall events, or may occur with no obvious external trigger, as the culmination of slow, long-term crack subcritical growth driven by gravitational stresses.



Figure 4: Conceptual sketch of time dependent rockfall initiation and examples of recorded rockfall impacts

Debris slides commonly occur on the talus slopes immediately upslope from walking tracks, or localised “hanging swamps” that have developed around the rim and middle benches of the escarpment cliffs. Collapse may be triggered by short, intense rainfall or prolonged wet periods that cause the soil to become saturated, reducing its effective shear strength. Failures often comprise a mixture of granular residual and colluvial soils, boulders, and vegetation (Figure 5). Slopes may show evidence of slow, long-term creep, with potential for sudden, rapid acceleration if pore pressures become sufficiently elevated to induce undrained failure.



Figure 5: Conceptual sketch and example of a debris slide in colluvium and residual soil

When debris slides initiate near creeks or ephemeral drainage lines along the crest of the escarpment, they can transition to channelised debris flows that entrain additional material along the runout path, producing a highly mobile, fluidised mixture of bouldery debris along with trees and surficial vegetation. Where drainage lines run over the crest of vertical cliff faces, the fluidised mass free-falls and may reach velocities exceeding 100 km/h. Recent debris flows in the Jamison Valley have produced runout distances of hundreds of metres; several were triggered by short, intense rainfall events during the La Niña weather conditions in the summers of 2020, 2021, and 2022 (Figure 6).

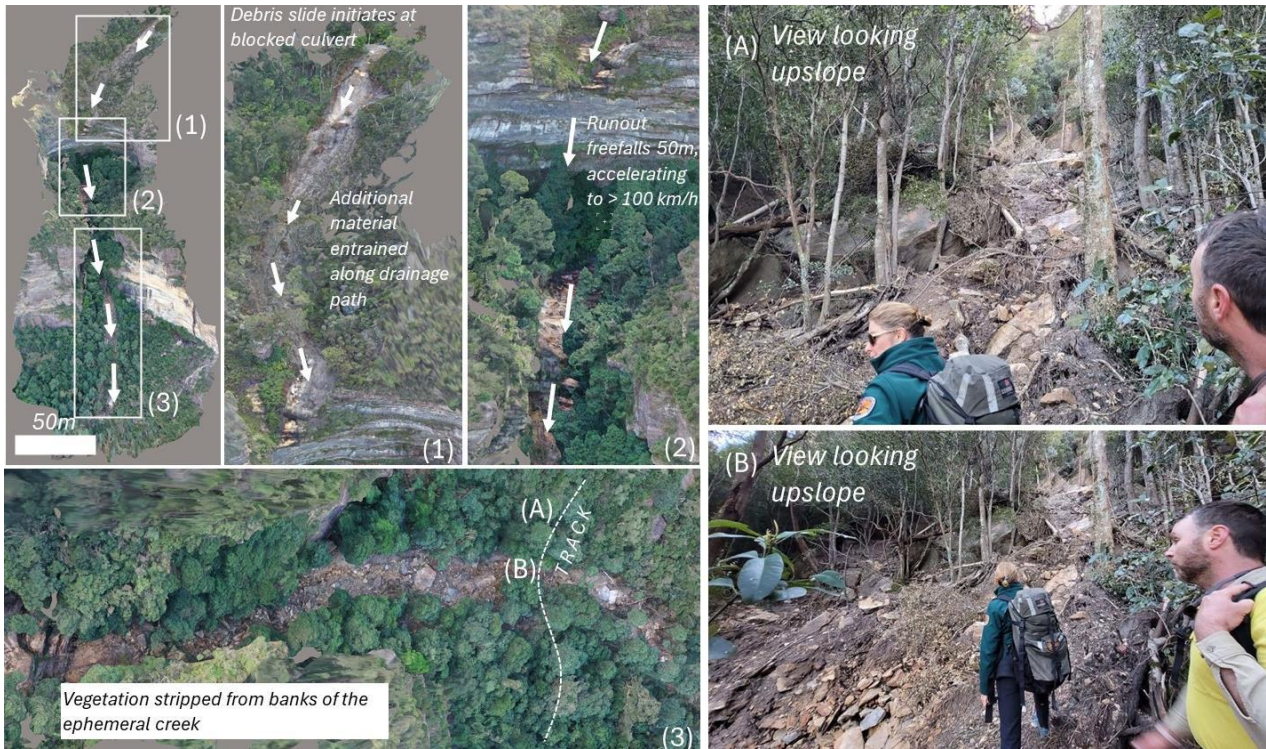


Figure 6: Example of a channelised debris flow in Jamison Valley (occurred in 2022)

A review of historical landslides undertaken for this study shows that the magnitude-frequency relationship appears to conform to a log-normal or negative exponential distribution, in agreement with published empirical trends observed in diverse geological environments around the world (e.g. Hungr et al., 1999). Most events comprise small, localised slumps or rockfalls with edge dimensions in the order of 1 m or less. However, there is also evidence for very large, deep-seated landslides with volumes in the millions of cubic metres. Figure 7 shows two examples including a recent multi-lobe debris slide on the southern flanks of Mount Solitary that occurred in early 2022, promoted by intense La Niña rainfall, and an ancient landslide at Carne Creek dated to 13,000 years, with estimated volume of 30 Mm³ (Tomkins et al., 2007).



Figure 7: Examples of very large recent and ancient rock and debris slides with volumes exceeding 1 Mm³

The Mount Solitary landslide was a low-consequence event because no walking tracks or other assets are near the runout path. However, other recent landslides have damaged walking tracks and critical fire trails, including a debris slide complex with volume in the tens of thousands of cubic metres that destroyed a section of Rodriguez Pass in Grose Valley in 2022. Previous QRA results for Rodriguez Pass, including consideration of risk to workers in re-establishing the trail through a landslide area, led NPWS to abandon the existing trail and develop an alternative access route into the valley.

The following sections introduce the concepts, methods, and results of the GIS landslide susceptibility and life risk mapping exercise. The landslide susceptibility rubric is specifically tailored to the landslide mechanisms described above, and the approach for estimating life risk uses empirical trends in landslide magnitude-frequency to link the landslide susceptibility score to an estimated “synthetic return period” for landslide initiation.

3 GIS LANDSLIDE SUSCEPTIBILITY MAPPING

3.1 LANDSLIDE SUSCEPTIBILITY CONCEPTS

Researchers and geoscience practitioners have published landslide susceptibility maps across a wide range of geological environments, resolutions, and scales. Caleca et al. (2025) presented a continental scale landslide susceptibility and risk mapping investigation spanning the European mountain ranges at 100 m resolution. Domínguez-Cuesta and Bobrowsky, (2013) produced a 1 km resolution Canada-wide landslide susceptibility map. Flentje et al. (2011) developed a 25 m² resolution qualitative landslide susceptibility map of the Sydney Basin. Smaller-scale examples include landslide susceptibility and hazard zoning maps produced for ski resorts in Kosciuszko National Park and the Victorian alpine region, and slope hazard zoning maps of the former Pittwater council (now part of Northern Beaches council) in Sydney; the production of these smaller-scale maps was initiated following the coronial enquiry into the Thredbo Landslide of 30 July 1997 (Leventhall and Kotze, 2008).

In broad terms, susceptibility describes the relative likelihood of landsliding. Common inputs into GIS-based landslide susceptibility maps include measurements of key terrain parameters such as slope angle, usually derived from a digital elevation model (DEM). Other spatial data may include bedrock and surficial geology units, gridded rainfall intensity data for a specific return period, vegetation cover and bushfire intensity mapping data, and proximity to watercourses (Corominas et al, 2014). Landslide inventory data may also be included, if the spatial extents of known or potential landslide features have been delineated through traditional geomorphology terrain analysis, or by using emerging techniques such as time-series change detection or machine-learning (Cochrane et al., 2024). Each of the input GIS datasets are assigned a weighted, numeric point score that contributes to the overall landslide susceptibility value. There is no universally accepted methodology for calculating landslide susceptibility, and the relative importance of each input dataset depends on site-specific engineering geology factors that control the expected landslide types. For this study, the landslide susceptibility “heat map” rubric was developed to consider the combined potential for the most common landslide failure mechanisms and impact scenarios:

- **Scenario 1:** A debris slide initiates at or near walking track level, with the source zone transporting downhill and potentially causing loss of the track or other asset. This scenario is particularly relevant for walking tracks that traverse across steep sections of the colluvial talus slopes.
- **Scenario 2:** A rockfall or debris slide initiates above the track and runs out onto the slopes below. This is the most common scenario for rockfall impacts to tracks that pass under the high escarpment cliffs. The likelihood of spatial impact is related to the “rockfall shadow” of the escarpment.

Figure 8 shows conceptual cross sections for both scenarios, along with corresponding examples of previous landslides where failure has either occurred near track level or involved runout of rockfalls initiating far above the track.

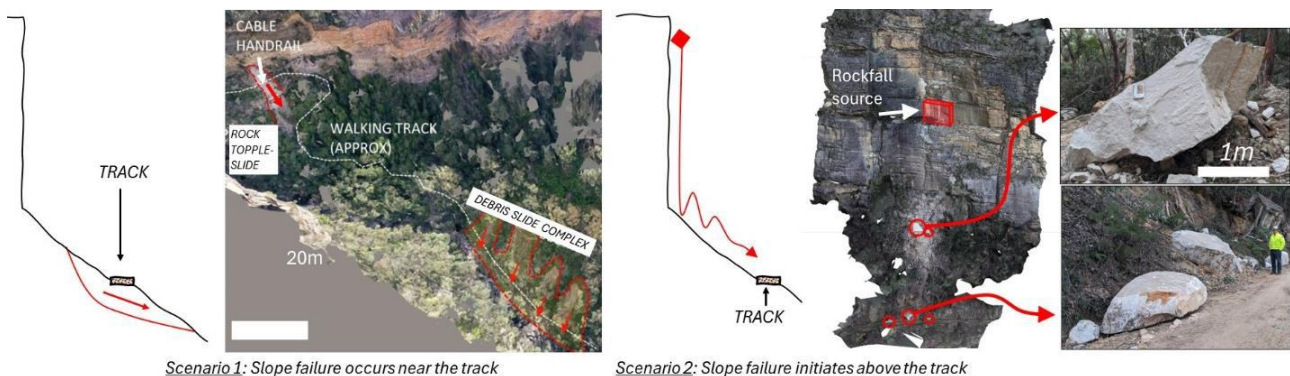


Figure 8: Landslide susceptibility combining the potential for localised instability and impact from above

3.2 GIS MAPPING METHODOLOGY

The landslide susceptibility scoring framework included five spatial input layers; these were selected based on data availability and expected correlation with the two landslide or rockfall impact scenarios described in the previous section. Data from each input layer were assigned a point score varying from 0 (nil susceptibility) to 100 (highest susceptibility). Weighting parameters were iteratively modified until the resultant “heat map” reflected the empirical evidence that most landslides and rockfalls occur in the immediate “rockfall shadow” of the escarpment cliffs and around the steepest sections of the valley side slopes, and incised creek channels. Table 1 summarises key details of each input data source.

Table 1: Summary of input GIS data and ranking for landslide susceptibility

Input Layer	Data Source (<i>Rationale</i>)	Data Range	Weighting
Horizon Angle	Publicly available LiDAR, 2 m resolution <i>Spatial likelihood of rockfall impact</i>	0 to 90°	35
Mean annual erosion using the Revised Universal Soil Loss Equation (RUSLE)	Modelled Hillslope Erosion over New South Wales, 100m resolution. Yang et al. (2017) <i>Shallow soil landslides triggered by rainfall</i>	0 to 25 t/ha/year	25
Slope Angle	Publicly available LiDAR, 2 m resolution <i>Soil or rock slide potential; runout distance</i>	0 to 90°	20
Rainfall IFD 7-day rainfall 50% AEP	Bureau of Meteorology, 2.5 km resolution <i>Orographic effects; higher rainfall areas are more susceptible to landsliding</i>	125 to 215 mm	15
Geology	NSW <i>Seamless Geology</i> (Colquhoun et al., 2022). <i>Weaker/more erodible units expected to correlate with increased frequency of landsliding</i>	Qualitative Point Ranking	5
Total Susceptibility Points			100

The “rockfall shadow” of the escarpment is a key factor influencing the potential for impact under Scenario 2 (rockfall initiation above the site). Proximity to the cliffs is quantified using the “horizon angle” measured from every pixel in the map to the highest point on the surrounding terrain. The horizon angle is analogous to the energy line, which is used to estimate rockfall kinetic energy with the cone method, where rockfall velocity v is calculated from the vertical distance Δh between any point on the terrain and the projected energy line (Castelli et al., 2021). Figure 9 illustrates the concept, showing how a track directly under the cliffs would have an apparent horizon angle approaching 90° and effectively 100% probability of spatial impact. Horizon angle and probability of spatial impact decrease with distance away from the cliffs.

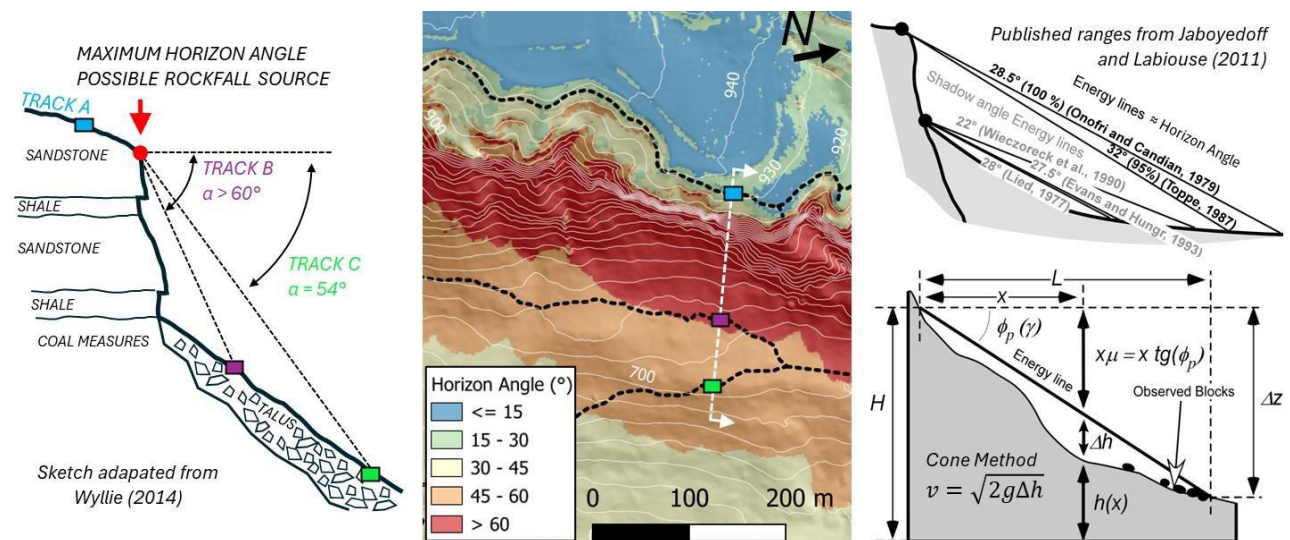


Figure 9: Illustration of the rockfall shadow concept, quantified by measuring maximum horizon angle

Empirical measurements of rockfall reach angle or Fahrböschung, measured from the source zone to the furthest runout block, can be used to develop a range of credible energy line values for a specific site (Field and Hunter, 2024). It is

important to note that the horizon angle is distinct from the “shadow angle”, which is instead measured from the apex of the talus slope (i.e. the base of the cliffs) to the furthest runout block (Evans and Hungr, 1993).

In summary, the susceptibility input weightings reflect the expectation that topography dominates the potential for landsliding. Geological map units are assigned the lowest relative weighting, accounting for only 5% of the total landslide susceptibility score. Qualitative point scores were assigned to each geological unit, with the highest susceptibility scores assigned to alluvial and colluvial soils. The relatively weaker coal measures rock units were assigned higher susceptibility scores than the overlying massive sandstones of the Narrabeen Group. Despite the limited influence assigned to the geological unit layer, the role of geology is implicitly accounted for in the DEM-derived terrain measurements, because present-day landforms are a product of long-term escarpment retreat processes which in turn are controlled by geology.

3.3 GIS MAPPING RESULTS

Figure 10 shows plan views of the five input layers and resultant project-wide “heat map” of landslide susceptibility. Each pixel in the landslide susceptibility map has a score varying from a minimum of 0 (negligible probability of landslide impact) to a maximum of 100 (worst-case, highest likelihood of landslide impact). The data were interrogated to develop qualitative landslide susceptibility classes varying from *low* to *very high* as a visualisation aid.

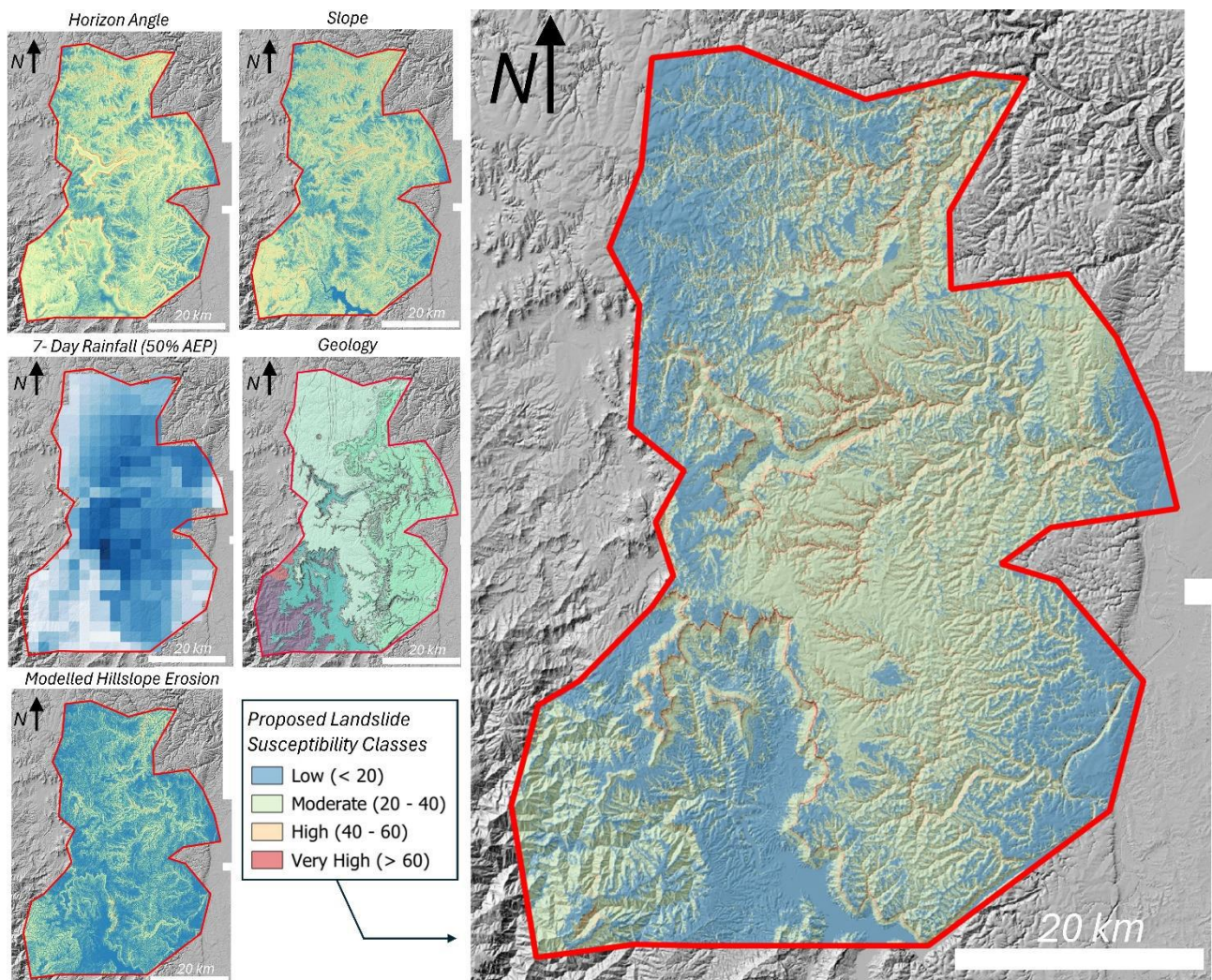


Figure 10: Plan view of input layers and resultant project wide “heat map” of landslide susceptibility

Linear assets including walking tracks and roads were split into 10 m long segments, with each segment assigned a single numeric landslide susceptibility score by sampling the maximum value from the underling heat map, within a 20 m wide buffer zone. An algorithm was developed to evaluate the terrain on either side of a track or road, and preferentially sample susceptibility values on the upslope side, to avoid very high landslide susceptibility scores for clifftop walking tracks that traverse near the upper crest of the escarpment. Figure 11 presents the resulting histograms and cumulative frequency curves of landslide susceptibility for the complete project-wide map (left), along with the corresponding results for

walking tracks (right). The statistics show that landslide susceptibility roughly conforms with a lognormal or negative exponential distribution, which is typical of many natural phenomena including landslide magnitude-frequency relationships (Hung et al., 1999). Under the proposed susceptibility classification framework, approximately 90% of the map area is assigned a *low* to *moderate* landslide susceptibility score. In contrast, 70% of walking track length falls into the *low* to *moderate* susceptibility classes; 22% of the total walking track length is subject to *high* landslide susceptibility and 8% of walking track length is subject to *very high* landslide susceptibility.

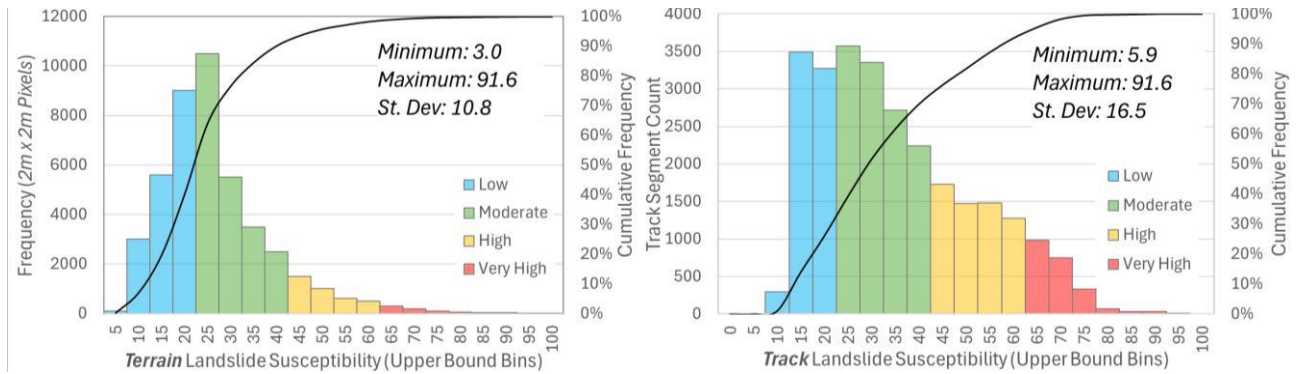


Figure 11: Histogram and cumulative frequency curves for landslide susceptibility of terrain and tracks

The data show that walking tracks are subject to higher landslide susceptibility than the overall terrain, reflecting the reality that these tracks have been constructed through steep terrain along the escarpment cliffs and upper reaches of the valley side slopes. The tracks with the highest landslide susceptibility include:

- **Cliffside tracks** that traverse along the base and intermediate benches of the escarpment cliffs. The most common slope failures affecting these tracks are expected to involve rockfalls initiating from the cliffs or overhangs, falling directly onto the walking track (no long-distance runoff is required).
- **Gully and slot canyon tracks** that pass through steep creek lines connecting the upper escarpment with the valleys below. The most common slope failures affecting these tracks are expected to involve debris flows and potentially rockfalls initiating from the rim of narrow slot canyons.
- **Valley tracks** that traverse along the base of the escarpment cliffs, across the steep upper talus slopes, such as Federal Pass and Wentworth Pass. The most common slope failures affecting these tracks are expected to involve debris slides initiating in over-steepened sections of the talus slope or cut slopes above the track, and debris flows following major rainfall events, impacting the tracks at creek and drainage line crossings.

3.4 LINKING LANDSLIDE SUSCEPTIBILITY TO LIFE RISK

Estimation of risk to life requires an annualised landslide return period (representing the QRA parameter P_H) and a temporal exposure parameter representing the probability that people will be present on the track or road when a landslide occurs (analogous to the QRA parameter P_r). Whereas susceptibility scores vary from 0 to 100, landslide return periods for a given site may vary from several per year, up to many thousands of years. To account for this variation, an exponential relationship was used to derive an artificial “synthetic return period” (SRP) from the susceptibility score, reflecting a similar trend to the negative exponential form of landslide magnitude-frequency data (e.g. Hunter et al., 2022). Figure 12 shows two proposed exponential relationships to estimate SRP from the underlying susceptibility score.

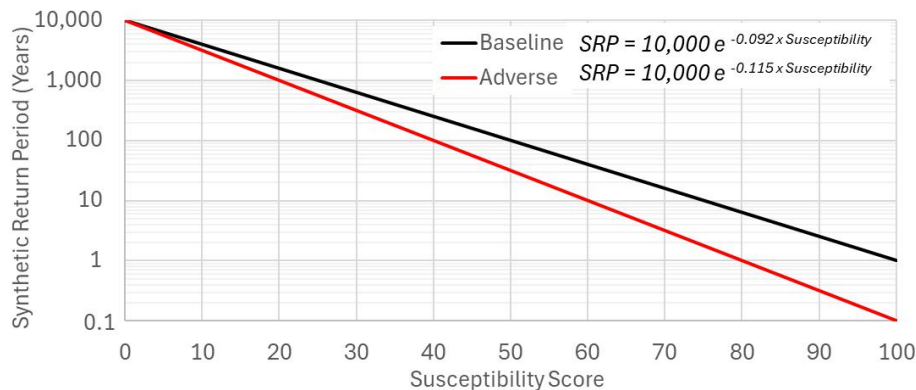


Figure 12: Proposed relationships between landslide susceptibility score and synthetic return period

Both SRP relationships assume a return period of 10,000 years for a susceptibility score of zero. The “baseline” relationship adopts an upper bound return period of 1 landslide per year for a score of 100. The “adverse” relationship adopts an upper bound return period of 0.1 years for a score of 100, corresponding to roughly one slope failure per month. It is important to note that the SRP estimates are not rigorously calibrated to historical landslide records, and they are not intrinsically linked to any specific failure mechanism or landslide size; rather, they have been selected to represent relative “base case” and “adverse” estimates of potential landslide frequency, for regional scale comparison of relative risk. In recent years, a new rockfall or landslide has been reported somewhere in the park about once per month. Many more landslides may occur in remote areas away from tracks and roads; furthermore, some fraction of rockfalls will either overshoot a track or road, or may come to rest on the slopes above the track, and thus go undetected.

Temporal exposure for park visitors was calculated for every track segment using annual visitation data provided by NPWS. Walkers were assumed to be travelling at 3 km/h through a notional “impact zone” that could vary in size from 1 m for a small rockfall, up to larger slope failures which could impact a complete 10 m long track segment. After calculating the synthetic QRA parameters for each track segment, the relative life risk can be interrogated in terms of a “synthetic fatality return period” with roads and tracks colour-coded to highlight the highest risk locations, accounting for both (1) landslide susceptibility; and (2) track visitation and the corresponding temporal exposure. Figure 13 shows an extracted map near Katoomba, with terrain coloured by landslide susceptibility, and tracks coloured by “synthetic life risk” categories under baseline conditions, for a landslide impacting a full 10 m track segment.

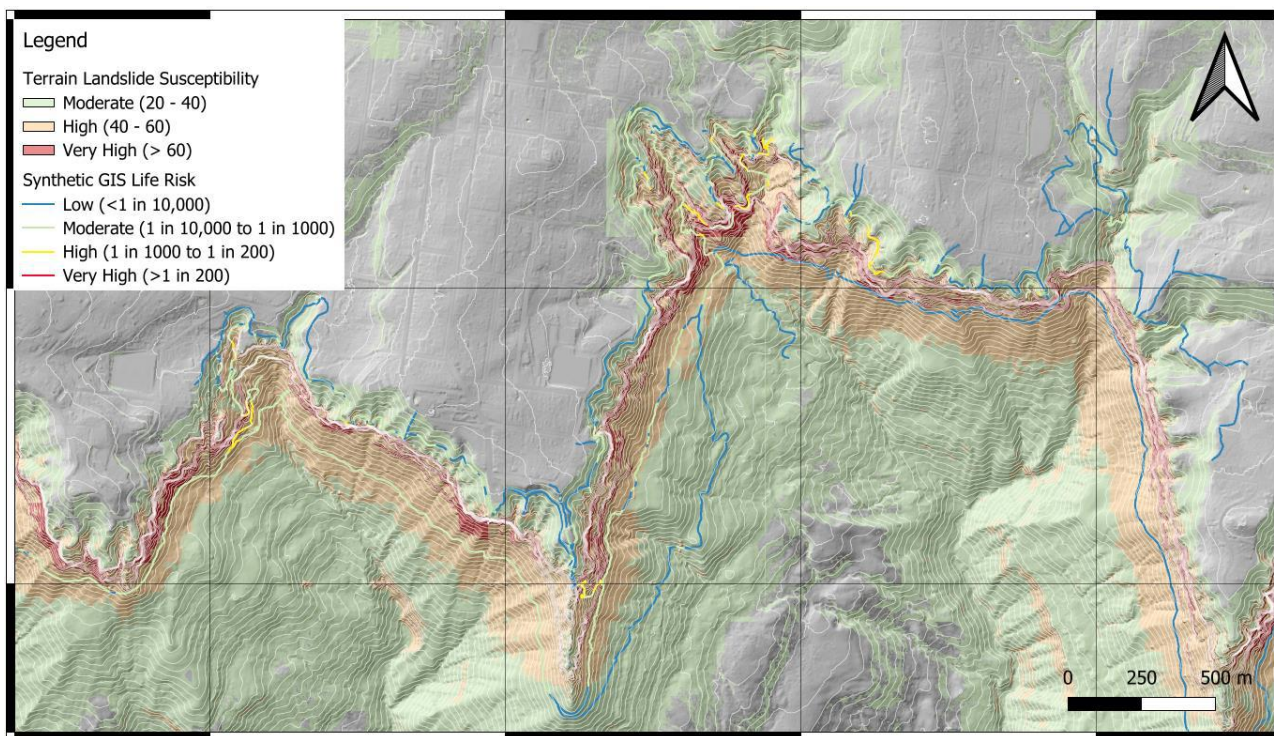


Figure 13: Tracks coloured by synthetic life risk, overlain on landslide susceptibility raster

Based on the proposed GIS risk classes, and considering a landslide that impacts a full 10 m long track segment, the walking track dataset is classified as 97.6% low to moderate life risk by track length. Only 2.3% of walking track length is classified as high life risk, and less than 0.1% falls into the very high life risk category.

4 DISCUSSION

Qualitative inspection of the regional scale mapping results confirmed that the high and very high risk areas broadly correspond with locations of known landslide impacts and high visitation; however, it must be emphasized that all estimates of life risk from this GIS analysis should be only used only to rank the relative risk of track and road assets and prioritise locations for site-specific investigation. The mapping results are intended to rapidly highlight the walking tracks and road sections subject to the highest life risk; they are not a conclusive determination of whether an asset is subject to tolerable or unacceptable societal risk in terms of the AGS (2007) risk assessment framework. In the near-term, the results will be used to highlight locations of high or very high risk where no previous geotechnical investigations have been undertaken and prioritise these areas for site-specific inspection and quantitative risk assessment.

There are several important limitations to the methodology. Although the landslide susceptibility score considers the potential for both debris slide and rockfall impact, initiation triggers may differ depending on the failure mechanism. Whereas brittle rockfalls may initiate with little warning, as the culmination of slow, gravity-driven subcritical crack growth, debris slides are known to correlate with intense rainfall or prolonged wet weather, when walkers are less likely to be present. Consequently, post-processing workflows to estimate life risk must adopt different weighting parameters for the temporal exposure parameter $P_{T,S}$ to reflect the reduced likelihood that walkers will be present during wet weather.

Furthermore, this investigation defined landslide susceptibility as the potential for rockfall impact or localised instability of steep slopes: channelised debris flows are under-represented in the project wide susceptibility map. Preliminary investigations have demonstrated that hydrologic simulation techniques can be integrated into the GIS mapping methodology to highlight track sections subject to debris flow risk. Figure 14 shows an example from the Jamison Valley, where the accumulated flow depth for an input storm event is calculated using the publicly available 2 m resolution DEM. Track sections coloured by the simulated flood depth give a proxy indication of debris flow potential, showing a good match with two observed debris flows, and highlighting areas that may be impacted in the future.

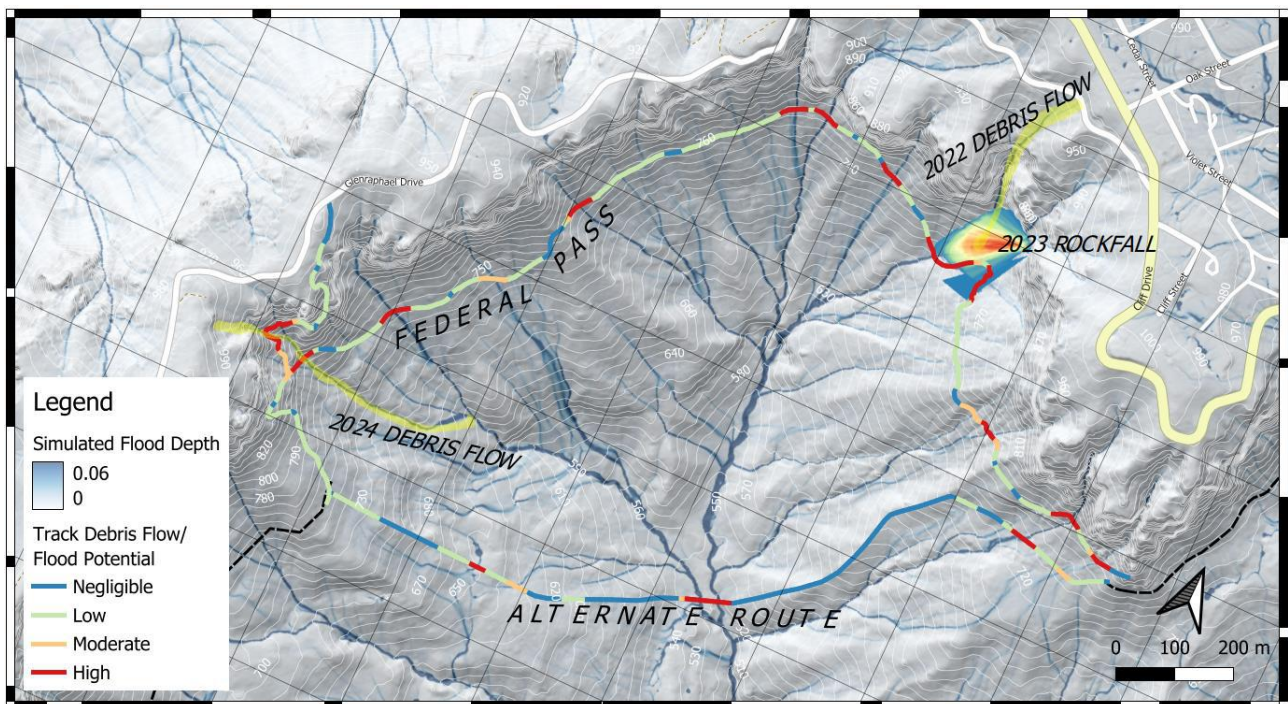


Figure 14: Example of a hydrologic simulation for overland flow to highlight creeks and drainage lines

Future developments could further improve confidence in the landslide susceptibility mapping by incorporating change detection techniques, with comparison of successive aerial LiDAR surveys. Over time, the landslide susceptibility scoring rubric can be refined to better reflect areas of real, observed instability.

5 CONCLUSIONS

This investigation produced a GIS database covering approximately 3400 km² of Blue Mountains National Park centred around the communities of Katoomba and Blackheath. The database includes topography and cadastral data, as well as a selection of five geospatial layers that were used to estimate susceptibility to impact from rockfalls and debris slides. The GIS database is hosted on a web viewing portal that allows NPWS to view the maps, interrogate the data, and generate localised plans as needed for areas of planned track work, or as part of the incident response to reported landslides.

A “synthetic return period” approach can be used to link landslide susceptibility to life risk based on the negative exponential form of empirical landslide magnitude-frequency data. The resulting heat maps of landslide susceptibility and life risk reflect the empirical observation that landslide susceptibility is highest near the steep escarpment cliffs, and on the steepest sections of the valley side slopes and incised creek channels.

6 REFERENCES

Australian Geomechanics Society (AGS) (2007). Practice note guidelines for landslide risk management. *Australian Geomechanics Journal*, 42(1), 63-114.

- Caleca, F., Lombardo, L., Steger, S., Tanyas, H., Raspini, F., Dahal, A., Nefros, C., Mărgărint, M.C., Drouin, V., Jemec-Auflič, M. and Novellino, A. (2025). Pan-European landslide risk assessment: From theory to practice. *Reviews of Geophysics*, 63(1).
- Castelli, M., Torsello, G. and Vallero, G. (2021). Preliminary modeling of rockfall runout: Definition of the input parameters for the QGIS plugin QPROTO. *Geosciences*, 11(2), 88-114.
- Cochrane, M., Cheesman, B., Pyke, A., and Kelly, R. (2024). Creation of city-scale landslide susceptibility maps using machine learning. In: *Proceedings of the Australian Geomechanics Society Symposium (Sydney Chapter)*, November 2024.
- Colquhoun G.P., Hughes K.S., Deyssing L., Ballard J.C., Folkes C.B, Phillips G., Troedson A.L. & Fitzherbert J.A. (2022). New South Wales Seamless Geology dataset, version 2.2 [Digital Dataset]. Geological Survey of New South Wales, Department of Regional NSW, Maitland.
- Corominas, J., van Westen, C., Frattini, P., Cascini, L., Malet, J.P., Fotopoulou, S., Catani, F., Van Den Eeckhaut, M., Mavrouli, O., Agliardi, F. and Pitilakis, K. (2014). Recommendations for the quantitative analysis of landslide risk. *Bulletin of engineering geology and the environment*, 73, 209-263.
- Cunningham, D.M. (1988). A rockfall avalanche in a sandstone landscape, Nattai North, NSW. *Australian Geographer*, 19(2), 221-229.
- Domínguez-Cuesta, M.J. and Bobrowsky, P.T. (2013). Proposed landslide susceptibility map of Canada based on GIS. *Landslide Science and Practice: Volume 3: Spatial Analysis and Modelling*, 375-382.
- Evans, S.G. and Hungr, O. (1993). The assessment of rockfall hazard at the base of talus slopes. *Canadian Geotechnical Journal*, 30(4), 620-636.
- Field, D. and Hunter, A. (2024). Methods for assessing remote rockfall hazards above transport corridors. *Australian Geomechanics Journal*, 59(3), 75-97.
- Flentje, P., Stirling, D. and Chowdhury, R. (2011). Landslide inventory, susceptibility, frequency and hazard zoning in the Wollongong and wider Sydney Basin Area. *Australian Geomechanics Journal*, 46(2), 41-49.
- Hatherly, P. and Brown, I. (2022). *The Blue Mountains: Exploring Landscapes Shaped by the Underlying Rocks, Uplift and Erosion*. Windy Cliff Press.
- Hungr, O., Evans, S.G. and Hazzard, J. (1999). Magnitude and frequency of rock falls and rock slides along the main transportation corridors of southwestern British Columbia. *Canadian Geotechnical Journal*, 36(2), 224-238.
- Hunter, A., Flentje, P., and Moon, A. (2022). Bulli Pass Landslide Risk Management Part 1 – Hazard Assessment. *Australian Geomechanics Journal*, 57(3), 97-113.
- Jaboyedoff, M. and Labiouse, V. (2011). Preliminary estimation of rockfall runout zones. *Natural Hazards and Earth System Sciences*, 11(3), 819-828.
- Leventhal, A.R. and Kotze, G.P. (2008). Landslide susceptibility and hazard mapping in Australia for land-use planning—with reference to challenges in metropolitan suburbia. *Engineering Geology*, 102(3-4), 238-250.
- NSW National Parks and Wildlife Service (2019). *Landslides and Rockfalls Procedures*. NSW Department of Planning, Industry and Environment, Sydney NSW.
- Pells, P.J.N., Braybrooke, J.C., Mong, J. and Kotze, G.P. (1987). Cliff line collapse associated with mining activities soil slope instability and stabilization. In: *Soil Slope Instability and Stabilisation*; Walker & Fell (Eds.), Balkema, Rotterdam, 359-385.
- Tomkins, K.M., Humphreys, G.S., Macris, J., and Hesse, P. (2007). Landslides in the Sydney basin: is there a seismic link. In: Clark, D. (Ed.) *Potential geologic sources of seismic hazard in the Sydney Basin. Proceedings volume of a one day workshop*, Geoscience Australia Record 2009/11 (GeoCat # 65991), 100-108.
- Tuckey, Z. (2023). The role of progressive brittle fracture in the 1931 landslide at Dogface Rock, Katoomba. *Australian Geomechanics Journal*, 58(3), 77-93.
- Wyllie, D.C. (2014). *Rock fall engineering*. CRC Press.
- Wyllie, D.C. and Mah, C. (2005). *Rock slope engineering*. CRC Press.
- Yang, X., Gray, J., Chapman, C., Zhu, Q., Tulau M., McInnes-Clarke, S. (2017). Digital mapping of soil erodibility for water erosion in New South Wales, Australia. *Soil Research*. 56(2), 158-170.